Biomicrofluidics

# An ultra-thin, all PDMS-based microfluidic lung assist device with high oxygenation capacity

Cite as: Biomicrofluidics **13**, 034116 (2019); https://doi.org/10.1063/1.5091492
Submitted: 02 February 2019 . Accepted: 11 June 2019 . Published Online: 27 June 2019

Mohammadhossein Dabaghi, Neda Saraei, Gerhard Fusch, Niels Rochow, John L. Brash, Christoph Fusch, and P. Ravi Selvaganapathy

Biomicrofluidics ARTICLE scitation.org/journal/bmf

# An ultra-thin, all PDMS-based microfluidic lung assist device with high oxygenation capacity

Cite as: Biomicrofluidics 13, 034116 (2019); doi: 10.1063/1.5091492
Submitted: 2 February 2019 · Accepted: 11 June 2019 ·
Published Online: 27 June 2019



Mohammadhossein Dabaghi,[1] Neda Saraei,[2] Gerhard Fusch,[3] Niels Rochow,[3] John L. Brash,[1,4] Christoph Fusch,[1,3,5] and P. Ravi Selvaganapathy[1,2,a)]

## AFFILIATIONS

[1]School of Biomedical Engineering, McMaster University, Hamilton, Ontario L8S 4L7, Canada
[2]Department of Mechanical Engineering, McMaster University, Hamilton, Ontario L8S 4L7, Canada
[3]Department of Pediatrics, McMaster University, Hamilton, Ontario L8S 4K1, Canada
[4]Department of Chemical Engineering, McMaster University, Hamilton, Ontario L8S 4K1, Canada
[5]Department of Pediatrics, Paracelsus Medical University-Nuremberg, University Hospital, Nuremberg 90419, Germany

[a)]**Author to whom correspondence should be addressed:** selvaga@mcmaster.ca

## ABSTRACT

Preterm neonates with immature lungs require a lung assist device (LAD) to maintain oxygen saturation at normal levels. Over the last decade, microfluidic blood oxygenators have attracted considerable interest due to their ability to incorporate unique biomimetic design and to oxygenate in a physiologically relevant manner. Polydimethylsiloxane (PDMS) has become the main material choice for these kinds of devices due to its high gas permeability. However, fabrication of large area ultrathin microfluidic devices that can oxygenate sufficient blood volumes at clinically relevant flow rates, entirely made of PDMS, have been difficult to achieve primarily due to failure associated with stiction of thin PDMS membranes to each other at undesired locations during assembly. Here, we demonstrate the use of a modified fabrication process to produce large area ultrathin oxygenators entirely made of PDMS and robust enough to withstand the hydraulic conditions that are encountered physiologically. We also demonstrate that a LAD assembled from these ultrathin double-sided microfluidic blood oxygenators can increase the oxygen saturation level by 30% at a flow rate of 30 ml/min and a pressure drop of 21 mm Hg in room air which is adequate for 1 kg preterm neonates. In addition, we demonstrated that our LAD could withstand high blood flow rate of 150 ml/min and increase oxygen saturation by 26.7% in enriched oxygen environment which is the highest gas exchange reported so far by any microfluidic-based blood oxygenators. Such performance makes this LAD suitable to provide support to 1 kg neonate suffering from respiratory distress syndrome.



## INTRODUCTION

Mechanical ventilation and extracorporeal membrane oxygenation (ECMO) are the two main options to provide additional oxygenation for preterm neonates with respiratory distress syndrome (RDS). Both methods are invasive and lead to long-term complications such as bronchopulmonary dysplasia.[1,2] In the first method, positive applied pressure in mechanical ventilation can cause damage to the baby's fragile lung tissues. Alternatively, current ECMO devices require a high blood volume to be primed (usually more than 20 ml), external pump, and oxygen supply.[3] An external pump could damage red blood cells and therefore lead to hemolysis.[4,5] Moreover, using oxygen as a sweep gas can limit the device portability. Therefore, a pumpless device, capable of being operated solely by the baby's heart (20–60 mm Hg) and with the ability of oxygenation in ambient air would be the best solution to minimize post-treatment side effects[3,5,6] (such a concept is known as an artificial placenta). Over the last years, several microfluidic-based devices have been introduced for blood oxygenation,[5,7–21] but only few of them[5,11,12,20] could be operated without any pump and have sufficient gas exchange capability in room air. Therefore, an ideal device for artificial placenta application should have (1) an ability to operate at a pressure differential of 20–60 mm Hg; (2) an ability to be oxygenated in ambient air; (3) a priming volume of <10 ml/kg of the body weight and the ability to process 20–30 ml/min/kg of blood and increase oxygen saturation of ∼30%, thereby an oxygen transfer of 1.3–1.9 mL/min/kg of body weight.[3–5,11,12,20]

Fabrication of microfluidic blood oxygenators with double-sided gas exchange[12,21] has led to promising improvement in performance lately. Two different approaches have been taken to fabricate such oxygenators, namely, (1) the use of gas perfusion channels on each side of the microfluidic blood network microchannels which provide mechanical support during the operation[21] or (2) the use of a stiffer material such as stainless-steel mesh to reinforce the PDMS gas exchange membrane[12] such that they could be directly exposed to the ambient atmosphere.[4] The first approach needs an external gas supply and pumps to perfuse the gases which is not desired, while the second approach reduces the effective gas exchange surface area due to the reinforcement that does not have the same permeation characteristics as PDMS. The reinforcement helps maintain the integrity of the gas exchange membrane both during the fabrication as well as during the operation and makes the device more reliable. Nevertheless, gas exchange efficiency can be considerably improved if the reinforcement were eliminated. It would be ideal to reliably fabricate large area, all PDMS, thin microfluidic device with gas exchange membrane on two sides that could be sufficient to provide the oxygenation capacity for 1 kg neonate while still reliably operating under physiological conditions. In this paper, we have adapted a technique to form conformal slippery surfaces[22–27] to coat the molds in order to form and release large area ultrathin PDMS layers embedded with microfluidic channel network. Using this method, we demonstrate the manufacture of a free standing double-sided single oxygenator unit (dsSOU) with a large surface area of 62.56 $cm^2$. Subsequently, we assembled 8 dsSOUs together as a LAD with minimum connectors and two flow distributors with the biomimetic design. Consequently, this LAD showed a high gas exchange capacity, even in room air which meets the minimum requirements for 1 kg preterm neonates. The experimental results demonstrated that this configuration is well suited for the passive pumpless operation for artificial placenta-type application in room air or oxygen-enriched environment.

## METHODS

### Design of dsSOU

The design for the dsSOUs consisted of the blood vascular network which is a layer of interconnected microchannels made by two thin nonporous PDMS membranes as shown in Fig. 1(a). The top and the bottom membranes had a thickness of 120 and 30 $\mu$m, respectively. The blood vascular network was square-shaped with a length of 91 mm [Fig. 2(b)] and a height of 160 $\mu$m [determined to

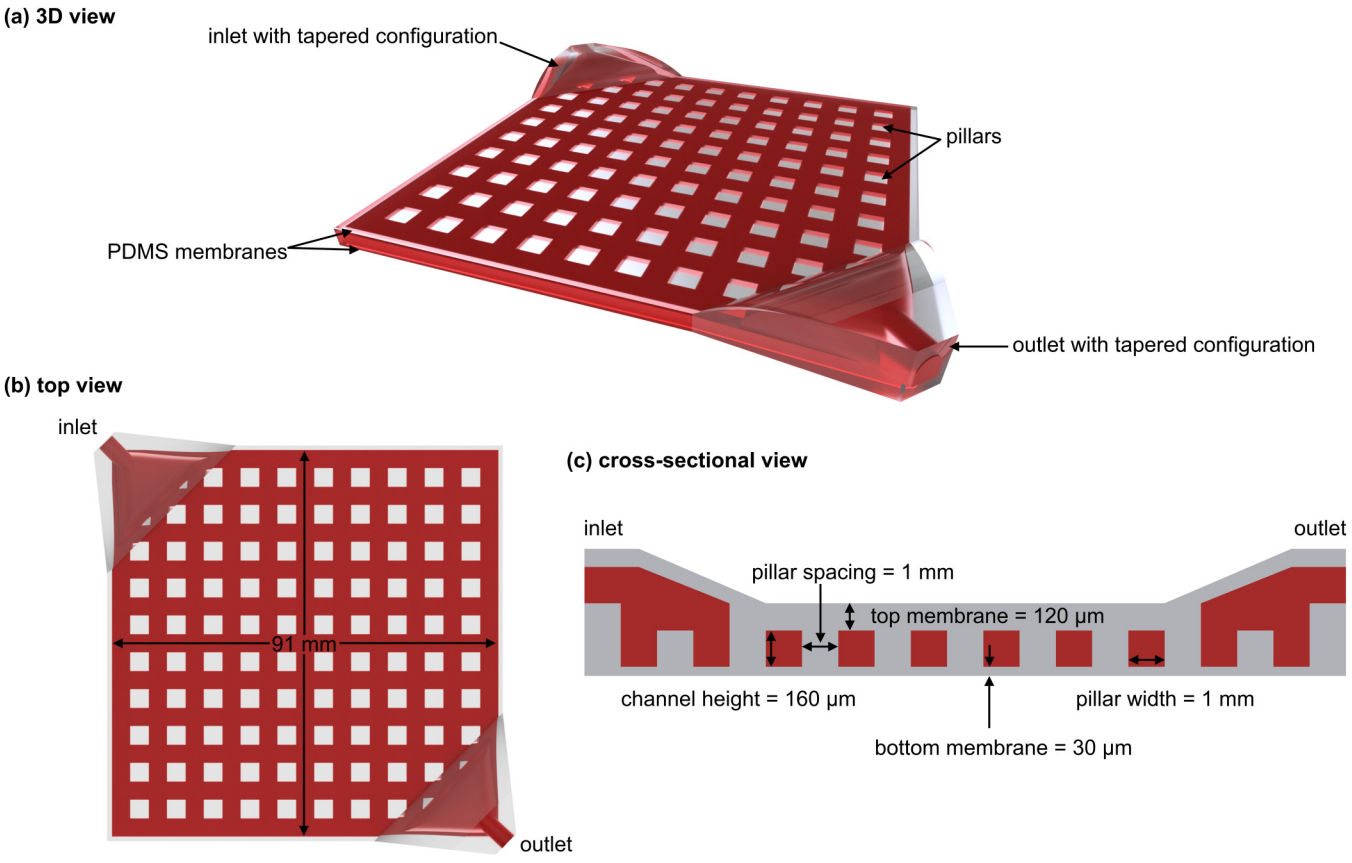


**FIG. 1.** (a) 3D schematic drawing of dsSOU with the tapered inlet configuration, (b) top view of dsSOU, and (c) the cross-sectional view of the device.

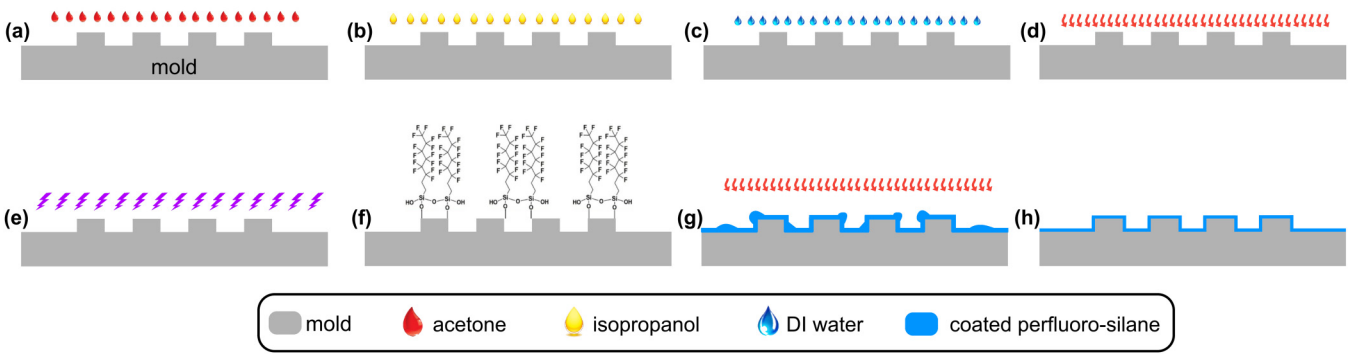


**FIG. 2.** Coating process for trichloro (1H 1H 2H 2H-perfluorooctyl) silane on the mold by CVD: (a) acetone treatment, (b) isopropanol treatment, (c) washing using DI water, (d) drying, (e) plasma treatment, (f) silane functionalization, (g) coating of perfluorosilane, and (h) removal of excess.

be optimal for the pumpless operation by numerical simulation described in Fig. S1(a) in the supplementary material]. An array of pillars with a dimension of $1 \times 1\,mm^2$ was placed (a spacing of 1 mm) inside the chamber to support the large area membranes, holding them apart [Fig. 1(b)] and thus forming the microchannel network. The pillar dimension and channel height were optimized in such a way to achieve a uniform velocity profile, low pressure drop, and low shear stress as demonstrated in Figs. S1(b)–(d) in the supplementary material. The thickness of the top membrane was optimized to provide sufficient structural strength for handling the device and to minimize membrane deflection, while the bottom membrane was optimized for high gas exchange which resulted in the different thicknesses chosen.

As pressure drop is one of the key factors for designing an artificial placenta-type oxygenator,[12] we developed a new inlet configuration (Fig. 1) for our devices to ameliorate the loss of pressure and shear stress generated at these locations. Inlets perpendicular to the microfluidic layer are typically used in many oxygenator designs as they are convenient and simple to fabricate. However, this particular type of access results in a significant redirection of blood which can introduce a large pressure drop. To address this issue, a tapered inlet configuration was designed which provided an access to the blood vascular network from the side of the blood channels. Moreover, a numerical simulation was performed to study the impact of the new inlet configuration on shear stress and pressure drop using the model which shows significant reduction in pressure drops and shear stress [explained in Figs. S1(e) and S1(f) in the supplementary material].

## Mold fabrication and coating

The negative mold for the blood vascular network was fabricated by the conventional photolithography using SU8 (3035, MicroChem). Chemical vapor deposition (CVD) method was used to coat a thin and uniform layer of a silane-based compound on a silicon-mold to reduce the stickiness of PDMS to the mold. First, the microfabricated mold was soaked in acetone for a minute [Fig. 2(a)] following by soaking in isopropanol for another minute [Fig. 2(b)] and then rinsing with de-ionized (DI) water [Fig. 2(c)]. Then, it was dried with compressed air and placed on a hot-plate at 150 °C for 15 min [Fig. 2(d)]. Next, it was exposed to oxygen plasma (900 mTorr, Harrick Plasma cleaner) for 2 min to activate its surface [Fig. 2(e)]. Then, it was placed under a desiccator besides a Petri dish containing a piece of kimwipe tissue which was wetted with 200 $\mu$l of trichloro (1H,1H,2H,2H-perfluorooctyl) silane (Sigma Aldrich) vacuumed to ~50 mm Hg [Fig. 2(f)]. After 1 h, it was taken out and placed on a hot-plate at 100 °C for 3 h to let unbonded silane molecules evaporate [Fig. 2(g)]. As a result, a uniform perfluorosilane was coated on the mold which resulted in an increase in the hydrophobicity of the surface to ~115° from 28° (shown in Fig. S2 in the supplementary material).

## Device fabrication process

To produce an ultrathin PDMS-based microfluidic blood oxygenator with double-sided microchannels, we modified our pervious device fabrication technique.[4,12] PDMS monomer and its curing agent was mixed with a ratio of 10:1 and desiccated to remove all air bubbles. PDMS was spin coated on top of the mold at a speed of 850 rpm for a minute and placed under a desiccator to remove air trapped inside hollow pillars' features in the mold [Fig. 3(a)]. It should be noted that this step was repeated few times till all hollow pillars' features in the mold filled with PDMS. An additional PDMS layer was spin coated at 1500 rpm for a minute and a frame of cellulose acetate membrane (to provide an annular support) was embedded into wet PDMS [Fig. 3(b)]. It was placed on a hot-plate at 85 °C for 30 min to cure PDMS and the membrane was peeled off from the mold [Fig. 3(c)]. In a next step, the bottom PDMS membrane was fabricated by spin coating PDMS on a substrate with a speed of 2000 rpm for a minute and was cured in an oven at 85 °C for 15 min [Fig. 3(d)]. An additional thin layer of PDMS (a thickness of ~2 $\mu$m) was spin coated on the cured PDMS membrane at a speed of 8000 rpm for a minute [Fig. 3(e)] to function as an adhesive layer. The blood vascular network and PDMS membrane were brought in contact and left at room temperature overnight [Fig. 3(f)]. Overnight curing let PDMS diffuse to both sides and formed a very strong bonding. Premanufactured, PDMS-made inlets with a tapered configuration

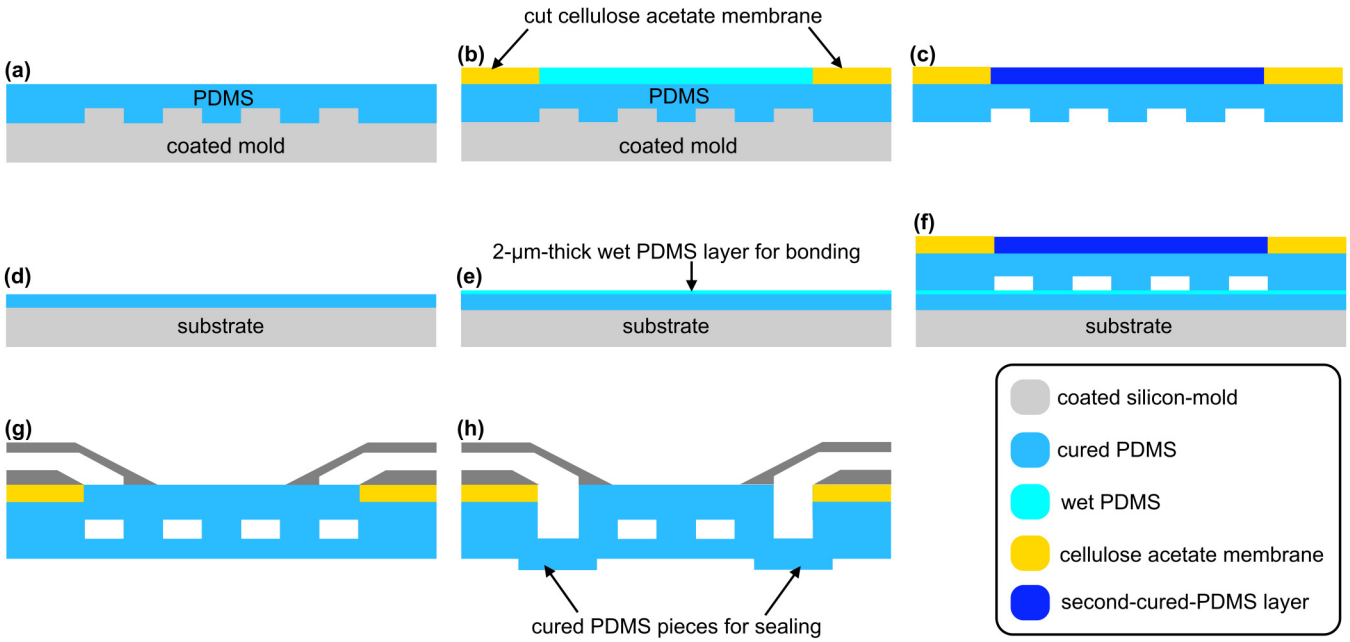


**FIG. 3.** Fabrication process for dsSOU with the tapered inlet configuration: (a) spin coating of first PDMS layer and its cure, (b) spin coating an additional thin PDMS layer and embedding cellulose acetate membrane, (c) cure of additional layer and peeling from the mold, (d) spin coating of the bottom PDMS membrane layer and its cure, (e) spin coating of a thin adhesive layer, (f) Integration of the bottom membrane with the top channel, (g) placement of inlet and outlet using half-cured PDMS, and (h) removal of residual PDMS and sealing the bottom side of each inlet/outlet.

were placed on two opposite corners using wet PDMS as a glue [Fig. 3(g)]. The bottom side of the blood vascular network (covered by the inlet/outlet) first was cut and residual PDMS was removed from the other side to open the inlet by a scalpel and a biopsy punch and two 1-mm-thick pieces of cured PDMS were used to seal the other sides [Fig. 3(h)].

The fabricated device with the tapered inlet/outlet configuration is shown in Fig. 4(a). This configuration spreads out the incoming blood into a larger area of the thin blood vascular network, and hence, produces a much smaller pressure drop and significantly smaller shear stress. In addition, its transparency can also be used to monitor any potential clot formation that may occur at this region. The cross section of one of the microchannels is shown in Fig. 4(b) in which the top and bottom membranes (thickness of 120 and 30 $\mu$m) can been seen clearly.

Burst pressure testing was performed on individual oxygenators to ensure that the bonding and PDMS membranes were strong enough. The fabricated oxygenators were found to withstand the operating pressure of 20–60 mm Hg easily and no failure was observed below 300 mm Hg. The process and the burst pressure results are shown in Fig. S3 in the supplementary material.

## Design criteria for LAD and its assembly

It should be noted that our LAD (an artificial placenta-type blood oxygenator) is designed for a parallel arterio–venous connection to the human circulatory system as opposed to conventional ECMO devices that are designed for a venous–artery or venous–venous configuration.[28] Therefore, in our configuration, blood entering the LAD is already partially oxygenated by the lung (arterial blood). As a result, our LAD is expected to operate at the upper end of the oxygen binding curve of hemoglobin compared to current ECMO devices and a typical increase in the oxygen saturation by 30% would be sufficient to fully saturate the incoming blood.[29] In addition, the priming volume of the LAD should be low enough so that no blood transfusion is needed.[30] To avoid cardiac output failure because of excessive bypass blood flow to the systemic circulation, the LAD should not be operated at very high blood flow rates. Consequently, blood flow rates should range from 20 to 30 ml/min/kg of a baby.[3,5,12,29,31] Therefore, LADs were tested with incoming blood saturation levels well below 70% (typically ~55%) in order to determine the full capacity of the oxygenator in increasing the saturation level at various operational flow rates.

In the construction of the LAD, eight dsSOUs were attached in parallel to meet the design criteria and to meet the estimated gas exchange needs of a preterm neonate weighing up to 2 kg. A parallel configuration was chosen here to increase the overall gas exchange capacity by operating the LAD at higher blood flow without making any discernible impact on the pressure drop or the oxygenation characteristics of devices. Flow distributors could provide symmetrical and biomimetic flow paths to blood without any damage to red blood cells (the hematocrit was measured before and after and did not change during the experiment). The branching channel design uses Murray's aw[32] which ensures a gentle flow

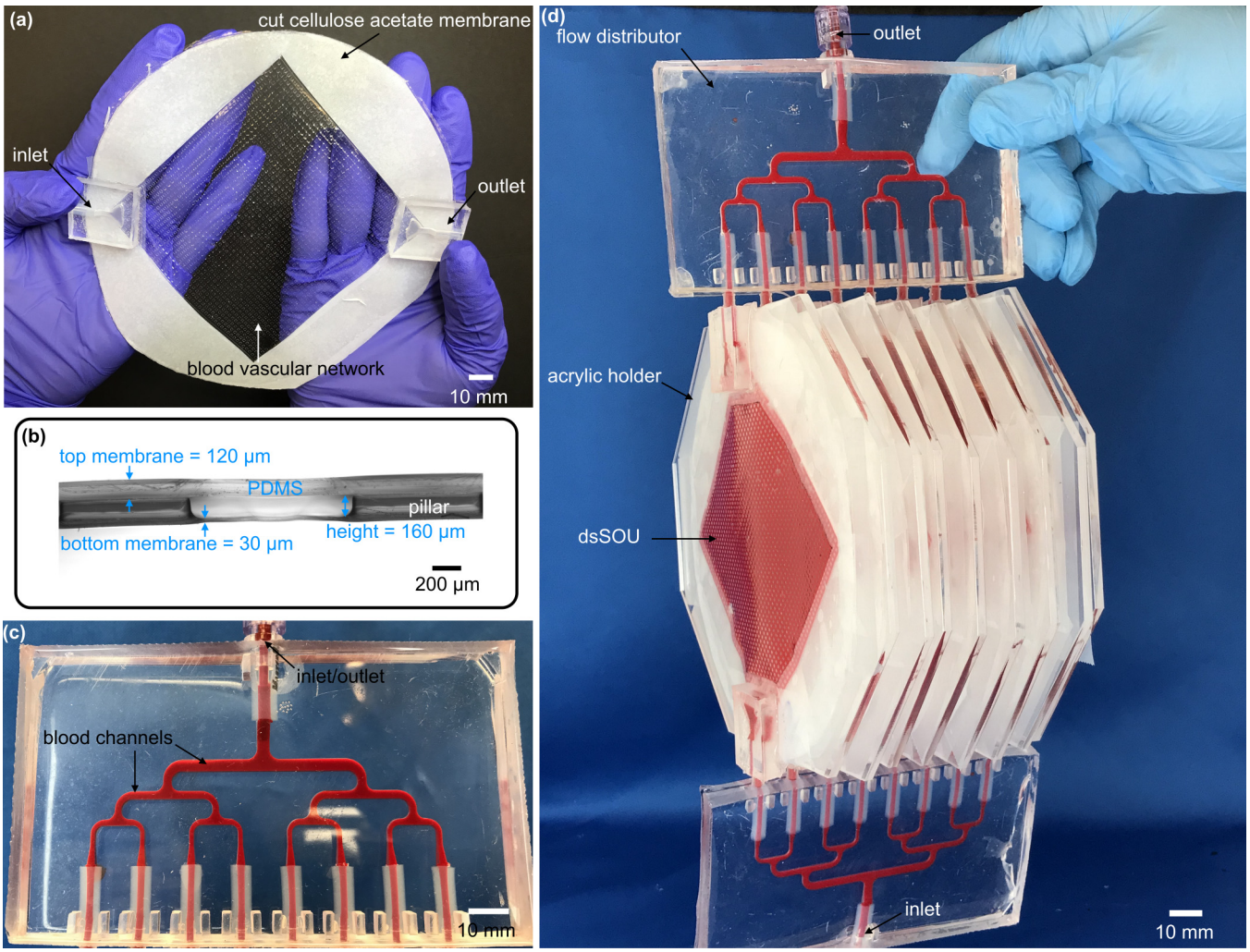


**FIG. 4.** (a) An image of dsSOU with the tapered inlet and outlet configuration, (b) a microscopic image cross-sectional view of the device, (c) the flow distributor filled with bovine blood, (d) the assembled LAD with 8 dsSOUs and two flow distributors which is filled with bovine blood.

distribution among channels without producing high pressure drop and shear stress and damaging red blood cells. To fabricate this flow distributor, the flow distributor was cast out of a 3D-printed mold (Formlab Form 2) and bonded to a cured PDMS using the flame-activation technique[33] as depicted in Fig. 4(c). Numerical simulations were performed to investigate the flow distribution uniformity, pressure drop, and shear stress profiles inside the flow distributors as seen in Figs. S1(g)–S1(i) in the supplementary material. These results illustrate that the flow distributors had a uniform velocity profile, a low pressure drop of ∼2 mm Hg at a blood flow rate of 60 ml/min, and a maximum shear stress of ∼6 Pa at the same blood flow rate. Attaching the dsSOUs to the flow distributors by connectors, the LAD was ready to test [Fig. 4(d)]. First, the LAD was perfused with normal saline solution and ran for 1 h to ensure that no device had a leakage.

## Experimental setup for the gas exchange testing with blood

Bovine blood (Bovine blood, sterile Citrated, CL1700-1000C) was purchased from Cedarlane and heparinized (3 U/ml). To be able to simulate partially saturated arterial blood conditions in the natural lungs, the oxygen saturation ($SaO_2$) level in blood was adjusted using a hollow fiber membrane oxygenator (PDMSXA-1.0, PermSelect®, Ann Arbor, MI) which was supplied by a carbon dioxide/nitrogen gas mixture (5%/95% v/v) in the fibers at 20 l/h. The blood was circulated with a flow of 15–25 ml/min through the oxygenator to reduce the oxygen saturation level to around 55 ± 5%. Once, the blood had reached the desired $SaO_2$, it was transferred to a bottle with a sealed lid and was stored in a fridge overnight to reduce the oxygen consumption by red blood cells (RBC) and achieve equilibrium.

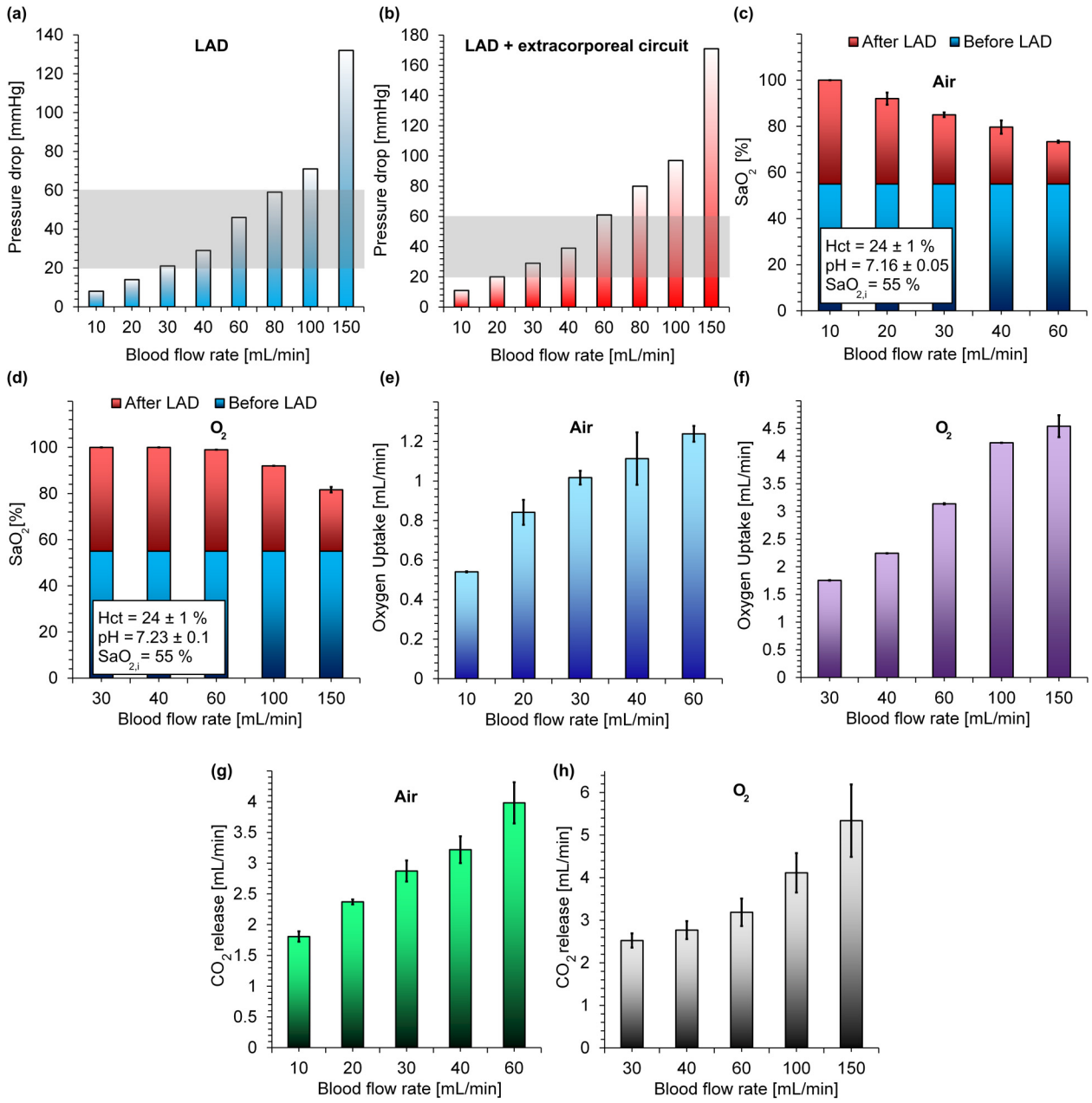


**FIG. 5.** *In vitro* performance of the LAD: (a) pressure drops of the LAD at various blood flow rates, (b) the pressure drop of the LAD plus the extracorporeal circuit at various blood flow rates, (c) oxygen saturation level before and after the LAD in room air oxygen at various blood flow rates, (d) oxygen saturation level before and after the LAD in an enriched oxygen environment at various blood flow rates, (e) oxygen uptake of the LAD in room air at various blood flow rates, (f) oxygen uptake of the LAD in an enriched oxygen environment at various blood flow rates, (g) $CO_2$ release of the LAD in room air at various blood flow rates, and (h) $CO_2$ release of the LAD in an enriched oxygen environment at various blood flow rates. Data represent the mean ± SD, $n = 3$.

The experimental setup is shown in Fig. S4 in the supplementary material. A TruWave Pressure Transducer (Edwards Lifesciences LLC, Irvine, CA) and a Spacelabs 90369 Patient Monitor (SpaceLabs Medical, Inc., Redmond, WA) were used to report the pressure drop during the experiment by installing the pressure transducer before the LAD. A point-of-care blood gas analyzer (GEM Premier 3000, Instrumentation Laboratory, Lexington, MA) was used in this study to measure blood properties before and after the device to

evaluate the gas exchanges by the device. In addition, a Complete MicroHematocrit System (StatSpin CritSpin, Norwood, MA) was used to measure the hematocrit level. To calculate the total content of oxygen in the blood, the amount of dissolved oxygen and the hemoglobin-bound oxygen were measured and summed.[20] For testing in room air, the LAD was exposed directly to ambient without any manifolds and the gas exchange measurements were done. For testing in an enriched oxygen environment at atmospheric pressure, the LAD was placed inside a Ziploc® bag and the bag was perfused with oxygen at a flow of 20 l/h (the bag was not fully sealed to let excess gases leave the bag). It should be noted that the hematocrit level before and after testing the LAD was monitored and no significant change was observed.

## RESULTS AND DISCUSSION

The performance of the LAD was assessed with bovine blood at blood flow rates between 10 and 60 ml/min in room air and between 30 and 150 ml/min in an enriched oxygen environment. The pressure drops of the LADs were also measured at various flow rates from 10 to 150 ml/min in two configurations: (1) only for the LAD and (2) the LAD with the extracorporeal circuit (the extracorporeal circuit includes all tubes before and after the LAD and all connectors used in the line) as shown in Figs. 5(a) and 5(b). The increase in the pressure drop with flow rates was found to be linear as expected and was within the operating pressure drop range [20–60 mm Hg, the gray box depicted in Figs. 5(a) and 5(b)] for blood flow rates below 60 ml/min, which satisfies the conditions for the pumpless operation of an artificial placenta-type oxygenator[12] while meeting the flow rates needed to support a 2 kg neonate.

Figure 5(c) shows the oxygen saturation level ($SaO_2$) in blood before and after the LAD at different blood flow rates in room air. The results showed that the oxygen saturation level of blood can be increased by 45% to 30% when the blood flow rate is between 10 and 30 ml/min. The level of saturation achieved is inversely correlated to the blood flow rate due to the fact that blood had smaller residence time in the LAD, and the red blood cells have a lower chance to adsorb oxygen molecules. In particular, the LAD was able to increase the oxygen saturation level by 30% at a blood flow rate of 30 ml/min and a low pressure drop of 21 mm Hg (29 mm Hg, including the extracorporeal circuit) which would satisfy the oxygenation need of a 1 kg preterm neonates with RDS.[5,12,20] In the case when the LAD was exposed to pure oxygen, it fully oxygenated blood (~100%) from 55% up to a flow rate of 60 ml/min as shown in Fig. 5(d). This level of increase in oxygen saturation level would be sufficient to support preterm neonates with RDS up to 2 kg in an artificial placenta format. It should be noted that, the LAD could achieve an oxygen saturation level of 92% (an increase in the saturation of 37%) even at a blood flow rate of 100 ml/min. These results suggest that this LAD configuration can support preterm neonates with various weights up to 2 kg with an oxygen ambient. The oxygen uptake in both conditions (room air and enriched oxygen environment) increased with the blood flow rate even up to 150 ml/min as more oxygen was carried by blood passing the LAD as shown in Figs. 5(e) and 5(f). For example, the oxygen uptake of the LAD at a blood flow rate of 30 ml/min was 1.01 and 1.75 ml/min in room air and oxygen, respectively. As the blood used in this experiment had low hematocrit content (as compared to that in neonate's blood), the calculated oxygen transfer underestimates the amount that would be transferred under similar conditions when a neonate's blood (with higher hematocrit) were used.

In addition, the carbon dioxide release that was calculated also increased with blood flow rates in both conditions as shown in Figs. 5(g) and 5(h). This behavior could be attributed to the decrease in the thickness of boundary layer close to both membranes at higher blood flow rates and to the increase in the total volume of $CO_2$ containing flowing across the membrane. Moreover, exposing the LAD to pure oxygen as compared to air did not have a significant effect on $CO_2$ release which is typical of many blood oxygenators. For instance, the $CO_2$ release of the LAD was $2.9 \pm 0.17$ ml/min and $2.55 \pm 0.16$ ml/min at a typical blood flow rate of 30 ml/min for an artificial placenta-type oxygenator.

Previous artificial placenta-type microfluidic-based oxygenator[12] have reported oxygen uptake of up to 2.86 ml/min (with a corresponding oxygen saturation level increased from 57% to 93%) at a blood flow rate of 60 ml/min using pure oxygen as the ambient

**TABLE I.** Comparison between this work and previous microfluidic blood oxygenator. All devices have been scaled to meet the requirement of an artificial placenta-type oxygenator in a pumpless manner (having a pressure drop of ~30 mm Hg). Number of single oxygenator units required to make an artificial placenta-type oxygenator is represented as $N_t$. Priming volume for only single oxygenator units and the total priming volume are shown by $PV_o$ and $PV_t$, respectively.

| Source | H ($\mu$m) | $N_t$ | Surface area ($cm^2$) | $PV_o$ (ml) | $PV_t$ (ml) | $\Delta SaO_2$ (%) | $O_2$ transfer (ml/min) | Blood flow (ml/min) | $\Delta P$ (mm Hg) | Gas |
|---|---|---|---|---|---|---|---|---|---|---|
| Hoganson *et al.*[18] | 100 | 5 | 115 | N/A | N/A | N/A | 0.48 | 31.5 | 20 | $O_2$ |
| Rochow *et al.*[5] | 80 | 20 | 305 | 2.5 | 10 | N/A | 1.04 | 30 | 32 | $O_2$ |
| | 80 | 20 | 305 | 2.5 | 10 | N/A | 0.61 | 30 | 32 | Air |
| Dabaghi *et al.*[12] | 200 | 4 | 250 | 5 | 8 | 42 | 1.96 | 30 | 30 | $O_2$ |
| Thompson *et al.*[13] | 30 | 6 | 189 | 2.8 | N/A | 38 | 1.13 | 30 | 33 | $O_2$ |
| Dabaghi *et al.*[4] | 160 | 3 | 300 | 3 | N/A | 40 | 1.89 | 30 | 30 | $O_2$ |
| This LAD | 160 | 8 | 800 | 8 | 12.5 | 30 | 1.01 | 30 | 21 | Air |
| | 160 | 8 | 800 | 8 | 12.5 | 45 | 1.8 | 30 | 21 | $O_2$ |
| | 160 | 8 | 800 | 8 | 12.5 | 45 | 2.24 | 40 | 29 | $O_2$ |

environment. In comparison, the new LAD in this work could achieve an oxygen uptake of 3.14 ml/min (raised oxygen saturation level from 55% to 99%) at the same blood flow rate but at a lower pressure drop (decreased by 13%). To be able to compare other microfluidic blood oxygenators[4,5,13,18] with the LAD developed in this study, their performance at a blood flow rate of ∼30 ml/min (which is required for a 1 kg preterm[5,12]) was determined and reported in Table I. An ideal device should increase oxygen saturation level by ∼30% at a maximum pressure drop of ∼30 mm Hg and a minimum blood flow rate of 30 ml/min in room air.[5,12,20] On this basis, the number of required single oxygenator units, total gas exchange surface area, priming volume, increase in oxygen saturation level, oxygen transfer, and blood flow rate has been calculated. The LAD in this study, achieves the highest increase in saturation (45%) with the lowest pressure drop (21 mm Hg) among all designs with oxygen as the exchange gas. Even using air as the exchange gas, it is able to demonstrate superior performance and achieves 30% increase in saturation at the lowest pressure drop of 21 mm Hg. Finally, the new LAD could achieve an oxygen transfer of 2.24 ml/min at a pressure drop of ∼30 mm Hg which is the highest among the listed devices in Table I operating in conditions to support a 1kg neonate in the artificial placenta format.

## CONCLUSION

In this paper, a LAD with eight microfluidic double-sided blood oxygenators was introduced which was capable of supporting higher blood flow rates with minimizing the priming volume of blood by using less connectors compared to other microfluidic blood oxygenators for preterm neonates with RDS. The device was made of two thin PDMS membranes on the top and the bottom of the blood flow path and had a high surface area for gas exchange. The use of perfluorosilane coating allowed the fabrication of an ultrathin PDMS-based microfluidic device for oxygenation purposes with high reliability. Gas exchange properties of this LAD were found to be better than other microfluidic-based oxygenators and were sufficient for preterm neonates. In the LAD construction, a biomimetic approach was taken to enhance the blood distribution and eliminate introducing dead zones and high shear stress regions. This LAD had a low priming volume of 12.5 ml and could provide a maximum oxygen transfer of 1.24 ml/min in room air and 4.54 ml/min using pure oxygen as ventilation gas. This LAD meets all design parameters of an artificial placenta-type device by having low priming volume, capable of being operated without the need of a pump, and capable of sufficient gas transfer in room air to support 1 kg neonate in the artificial placenta configuration. Such a LAD has a potential to be evaluated in animal experiments considering the fact that inner surface of the LAD which is PDMS can be easily cleaned by 70% ethanol without losing its functionality in gas transfer.

## SUPPLEMENTARY MATERIAL

See the supplementary material for the numerical modeling of shear stress and pressure drop in the device. It also describes the fabrication process of the tapered inlet, additional experiments characterizing the surface properties after the coating and burst pressure of the device as well as the experimental setup used for testing the device.

## ACKNOWLEDGMENTS

This work was supported by the Natural Sciences and Engineering Research Council of Canada (NSERC) and Canadian Institutes for Health Research (CIHR) through the Collaborative Health Research Program. P.R.S. also acknowledges the support from the Canada Research Chairs Program as well as the Discovery Accelerator Supplement grant. C.F. acknowledges the support from Jack Sinclair Chair funding.

## REFERENCES

[1]R. J. Rodriguez, Respir. Care **48**, 279 (2003), see http://rc.rcjournal.com/content/48/3/279.short.
[2]K. Fletcher, R. Chapman, and S. Keene, Semin. Perinatol. **42**(2), 68 (2018).
[3]N. Rochow, E. C. Chan, W.-I. Wu, P. R. Selvaganapathy, G. Fusch, L. Berry, J. Brash, A. K. Chan, and C. Fusch, Int. J. Artif. Organs **36**, 377 (2013).
[4]M. Dabaghi, N. Saraei, G. Fusch, N. Rochow, J. L. Brash, C. Fusch, and P. R. Selvaganapathy, Lab Chip **18**, 3780 (2018).
[5]N. Rochow, A. Manan, W. I. Wu, G. Fusch, S. Monkman, J. Leung, E. Chan, D. Nagpal, D. Predescu, J. Brash, P. R. Selvaganapathy, and C. Fusch, Artif. Organs **38**, 856 (2014).
[6]J. Peng, N. Rochow, M. Dabaghi, R. Bozanovic, J. Jansen, D. Predescu, B. DeFrance, S.-Y. Lee, G. Fusch, P. Ravi Selvaganapathy, and C. Fusch, Int. J. Artif. Organs **41**, 393 (2018).
[7]J. K. Lee, M. Kung, H. Kung, and L. Mockros, ASAIO J. **54**, 390 (2008).
[8]K. M. Kovach, M. A. LaBarbera, M. C. Moyer, B. L. Cmolik, E. van Lunteren, A. Sen Gupta, J. R. Capadona, and J. A. Potkay, Lab Chip **15**, 1366 (2015).
[9]A. A. Gimbel, E. Flores, A. Koo, G. García-Cardeña, and J. T. Borenstein, Lab Chip **16**, 3227 (2016).
[10]A. J. Thompson, L. H. Marks, M. J. Goudie, A. Rojas-Pena, H. Handa, and J. A. Potkay, Biomicrofluidics **11**, 024113 (2017).
[11]H. Matharoo, M. Dabaghi, N. Rochow, G. Fusch, N. Saraei, M. Tauhiduzzaman, S. Veldhuis, J. Brash, C. Fusch, and P. R. Selvaganapathy, Biomicrofluidics **12**, 014107 (2018).
[12]M. Dabaghi, G. Fusch, N. Saraei, N. Rochow, J. Brash, C. Fusch, and P. R. Selvaganapathy, Biomicrofluidics **12**, 044101 (2018).
[13]A. J. Thompson, L. J. Ma, T. J. Plegue, and J. A. Potkay, IEEE Trans. Biomed. Eng. **66**(4), 1082 (2019).
[14]K. A. Burgess, H. H. Hu, W. R. Wagner, and W. J. Federspiel, Biomed. Microdevices **11**, 117 (2009).
[15]D. M. Hoganson, J. L. Anderson, E. F. Weinberg, E. J. Swart, B. K. Orrick, J. T. Borenstein, and J. P. Vacanti, J. Thorac. Cardiovasc. Surg. **140**, 990 (2010).
[16]J. A. Potkay, M. Magnetta, A. Vinson, and B. Cmolik, Lab Chip **11**, 2901 (2011).
[17]T. Kniazeva, J. C. Hsiao, J. L. Charest, and J. T. Borenstein, Biomed. Microdevices **13**, 315 (2011).
[18]D. M. Hoganson, H. I. Pryor, E. K. Bassett, I. D. Spool, and J. P. Vacanti, Lab Chip **11**, 700 (2011).
[19]T. Kniazeva, A. A. Epshteyn, J. C. Hsiao, E. S. Kim, V. B. Kolachalama, J. L. Charest, and J. T. Borenstein, Lab Chip **12**, 1686 (2012).
[20]W.-I. Wu, N. Rochow, E. Chan, G. Fusch, A. Manan, D. Nagpal, P. R. Selvaganapathy, and C. Fusch, Lab Chip **13**, 2641 (2013).
[21]T. Rieper, C. Muller, and H. Reinecke, Biomed. Microdevices **17**, 1 (2015).
[22]A. Tuteja, W. Choi, J. M. Mabry, G. H. Mckinley, and R. E. Cohen, Proc. Natl. Acad. Sci. U.S.A. **105**(47), 18200 (2008).
[23]X. Li, D. Reinhoudt, and M. Crego-Calama, Chem. Soc. Rev. **36**, 1350 (2007).
[24]D. C. Leslie, A. Waterhouse, J. B. Berthet, T. M. Valentin, A. L. Watters, A. Jain, P. Kim, B. D. Hatton, A. Nedder, K. Donovan, E. H. Super, C. Howell,

C. P. Johnson, T. L. Vu, D. E. Bolgen, S. Rifai, A. R. Hansen, M. Aizenberg, M. Super, J. Aizenberg, and D. E. Ingber, Nat. Biotechnol. **32**, 1134 (2014).
[25]A. K. Epstein, T. Wong, R. A. Belisle, E. Marie, and J. Aizenberg, Proc. Natl. Acad. Sci. U.S.A. **109**, 13182 (2012).
[26]M. Villegas, Z. Cetinic, A. Shakeri, and T. F. Didar, Anal. Chim. Acta **1000**, 248 (2018).
[27]T. Wong, S. H. Kang, S. K. Y. Tang, E. J. Smythe, B. D. Hatton, A. Grinthal, and J. Aizenberg, Nature **477**, 443 (2011).
[28]E. P. Rivers, D. S. Ander, and D. Powell, Curr. Opin. Crit. Care **7**, 204 (2001).
[29]W. Tin, Arch. Dis. Child. Fetal Neonatal Ed. **84**, F106 (2001).
[30]R. Kopp, R. Bensberg, J. Arens, *et al.*, ASAIO J. **57**, 158 (2011).
[31]W. Wu, N. Rochow, G. Fusch, R. Kusdaya, A. Choi, P. R. Selvaganapathy, and C. Fusch, "Development of microfluidic oxygenators as lung assisting devices for preterm infants," presented at The 15th International Conference on Miniaturized Systems for Chemistry, Seattle, WA, 2–6 October 2011.
[32]C. D. Murray, Proc. Natl. Acad. Sci. U.S.A. **12**, 207 (1926).
[33]R. Ghaemi, M. Dabaghi, R. Attalla, A. Shahid, H.-H. Hsu, and P. R. Selvaganapathy, J. Micromech. Microeng. **28**, 087001 (2018).